Proceedings of the XIII International Conference "Ion Implantation and Other Applications of Ions and Electrons"

Ionization of Short-Lived Nuclides in the Hot Disc-Shaped Cavity

M. Turek*

Institute of Physics, Maria Curie Skłodowska University, Pl. M. Curie-Skłodowskiej 1, 20-031 Lublin, Poland

Doi: 10.12693/APhysPolA.142.761 *e-mail: mturek@kft.umcs.lublin.pl

The numerical model of ionization in disc-shaped cavities that takes into account both the radioactive decay of the nuclide and the delay of the emission due to the particle–wall sticking is presented. The dependences of ionization efficiency on timescales characterizing radioactive decay and sticking are presented and discussed. Two different cavity shapes are considered. One of them is a flat disc cavity, more suitable for stable or long-lived but hard-to-ionize isotopes. The other is a compact cavity, superior for short-lived nuclides, especially those easy-to-ionize. Average times the particle stay inside the cavity have been estimated — these times are more than an order of magnitude shorter in the case of a compact cavity. The influence of the extraction opening size on the efficiency of ionization in the flat disc cavity is discussed. It is shown that increasing this opening is an easy way to increase efficiency in the case of short-lived isotopes. The current–voltage curves calculated for both cavity configurations are presented. It is proved that the optimal extraction voltages for the compact and flat disc configurations are 0.5 kV and 2 kV, respectively.

topics: surface ionization, hot cavity ion sources, isotope on-line separation

1. Introduction

Hot cavity surface ionization ion sources entered the stage in the early seventies of the 20th century [1–3]. Nevertheless, their numerous advantages like robustness and reliability, simple maintenance, excellent beam quality (low energy spread and high purity), and last but not least, very high efficiency, as well as microamounts of feeding substance needed to obtain an ion beam, made these devices the "weapons of choice" in a variety of fields, especially nuclear spectroscopy [4, 5] and mass spectroscopy [6, 7]. Constructions based on such ion sources, sometimes having a form of resonant ionization laser ion sources (RILIS) [8–12], are often the cornerstones of a variety of ISOL (isotope separation on-line) facilities [13–17].

The basic part of a typical hot cavity ion source is a semi-opened ionizer, usually made of refractory metal (W, Ta, Mo). The ionizer is heated to a high working temperature ($\simeq$ 2500–3000 K or more) by electron beam bombardment [18] or ohmically [19]. In typical designs, the ion source is equipped with a target irradiated by a proton or heavy ion beam in order to produce isotopes of interest. The target and the ionizer are connected by a transfer line [20], but in some solutions, the ionizer itself could be the target [18]. The nuclides produced are immediately released into the hot cavity, which is an additional advantage in the case of short-lived species. A tubular ionizer is a typical solution. However, other shapes could be also found in some devices [21, 22].

A variety of theoretical models of ionization in hot cavities have been proposed over the years [23–26]. They were usually based on the assumption that neutral particles trapped in a cavity undergo multiple collisions with the inner hot surfaces, which leads to a large total ionization efficiency. The numerical model of ionization in hot cavities was presented in detail in the series of papers. Different shapes of ionizers were considered, i.e., tubular [27–30], spherical or hemispherical [31–33] as well as conical ones [34–36]. Early versions of the model were only suitable for stable nuclides, later on, the effects of radioactive decay and particle emission delays due to diffusion and effusion were included [32, 37]. In some cases (e.g., hard-to-ionize elements), electron impact ionization could also provide a very important contribution. Therefore, it was implemented in the numerical code [28, 29, 32]. Recently, a flat-disc cavity has been proposed [38], being a limiting case of a cylindrical ionizer, but characterized by a shorter length compared to its radius. The flat shape results in a larger number of particle–wall collisions

as the particles travel toward the extraction opening. It was shown that in the flat disc cavities, in the case of stable nuclides, the efficiencies of 90% can be achieved even for relatively hard-to-ionize substances.

In this paper, the ionization of short-lived nuclides in the flat-disc cavities is considered. A brief description of the model taking into account radioactive decay, and effusion delay losses is given for completeness. Two different shape configurations are investigated in the paper, one of which is more compact, and the other is a typical flat disc cavity. Changes of the ionization efficiency with the nuclide life-time are presented and discussed for both mentioned cavity shapes. There is also studied the role of effusion delays, namely changes in total efficiency with the average particle–wall sticking time for the different cavity shapes. The dependence of the ionization efficiency on the diameter of the extraction opening is also under investigation. The current–voltage curves calculated for different cavity configurations are shown and commented upon.

2. Numerical model

The numerical code is designed to determine the trajectories of neutrals and ions inside the disc-shaped cavity and calculate the ionization efficiency by counting the ratio of the number of desired particles as well as the number of all particles passing the extraction opening. This is a modified version of the code presented in previous papers [27–38]. A schematic view of the simulated system geometry is shown in Fig. 1. It should be reminded that a disc-like cavity is obtained when the diameter of the cavity $2r_i$ is larger than its length L. For the sake of simplicity, a flat extraction electrode on the negative potential V_{ext} is placed at the distance $d = 1$ mm from the outer rim of the extraction opening. The simulation area is covered by a 3D rectangular grid $(100 \times 400 \times 400)$ with the cell sizes $\Delta x = \Delta y = \Delta z = 0.05$ mm.

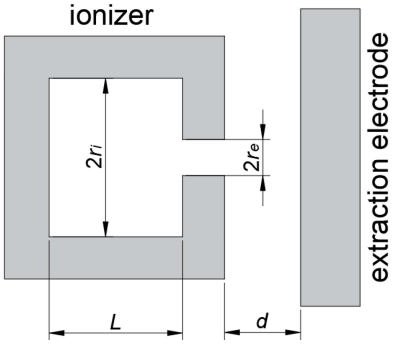

Fig. 1. Schematic view of the simulated system (r_i — internal radius of the ionizer, L — ionizer cavity length, d — distance between the ionizer and the extraction electrode, r_e — extraction opening radius).

The distribution of the electrostatic potential determined by all electrodes is found by numerical solving of the Laplace equation using the successive over-relaxation approach used, e.g., in other models [39–42]. The electric field is calculated by numerical derivation of the potential, and the forces pushing the particles are worked out by the interpolation of the values taken from the six mesh nodes nearest to the particle position. A well-established 4th order Runge–Kutta scheme is used to integrate the equations of motion. Within the model, the ionization/neutralization of particles touching the hot walls of the ionizer is taken into account based on the ionization probability β (sometimes referred to as the ionization coefficient) related to the ionization degree α using the formula

$$\beta = \frac{\alpha}{1+\alpha}. \tag{1}$$

The ionization degree is defined as the ratio of ions and neutrals leaving the surface. This quantity can be estimated using the famous Saha–Langmuir formula

$$\alpha = G \exp\left(-\frac{V_i - \phi_e}{k_{\mathrm{B}} T}\right), \tag{2}$$

where V_i and ϕ_e are the ionization potential and the work function of the ionizer material, respectively, T is temperature, and the factor G includes the particle–surface reflection coefficient as well as the statistical weights of ion and neutral atom ground levels.

As already mentioned, the upgraded model takes into account losses of the desired nuclide due to radioactive decay. It is assumed that the nucleus of each subsequent atom undergoes decay after some randomly chosen time

$$t_{\mathrm{dec}} = -\tau_{1/2} \ln(\mathrm{RND}), \tag{3}$$

where $\tau_{1/2}$ is the nuclide half-life and RND is a normal random number, i.e., taken from the range $(0, 1)$. It should also be stressed that particles adsorbed on a hot surface spend some finite time on it before they are detached. The time t_{stick} a particle stays on the ionizer wall is calculated for each collision using the formula

$$t_{\mathrm{stick}} = -\tau_s \ln(\mathrm{RND}), \tag{4}$$

where τ_s is the average particle sticking time for a given atom–surface combination. This quantity depends largely on the surface temperature, and some experimental values could be found, e.g., in [43]. The code registers all particles leaving the ionizer cavity, and the total ionization efficiency in the considered case is calculated according to the formula

$$\beta_s = \frac{N_{p+}}{N_{p+} + N_{s+} + N_{p0} + N_{s0}}, \tag{5}$$

where N_{p+} and N_{s+} are the numbers of ions of the primary (desired) and secondary ions, respectively, while N_{p0} and N_{s0} are the numbers of the corresponding neutral atoms passing the extraction opening.

3. Simulation results

In the first stage, the influence of the desired nuclide half-life on the ionization efficiency was investigated. Calculations were performed for two different ionizer cavity geometries. The first one, being a rather flat disc cavity, is characterized by $L = 1$ mm and $r_i = 7$ mm, while the second one is much more compact ($L = 1$ mm and $r_i = 1$ mm). The radius of the extraction opening is set to $r_e = 0.5$ mm unless otherwise stated, and the length of the extraction channel is $l = 0.2$ mm. The extraction voltage was set to $V_{ext} = 2$ kV.

The simulation timestep was $\Delta t = 0.01$ μs. Calculations were performed using 10^5 of test particles of mass 150 a.m.u.. The results presented in Fig. 2 were obtained for $\tau_s = 0$ (delays due to the sticking are neglected). As one can see, the ionization efficiency decreases with $\tau_{1/2}$. As in the previously considered cases of spherical [31–33] or conical cavities [34–36], this effect is of great importance when the average total time of the particle stay in the ionizer $\langle t \rangle$ is comparable to the nuclide half-life. As one can see in Fig. 3, the average flight time $\langle t \rangle$ without delays due to sticking varies from 2 ms down to 1 μs in the case of a flat disc cavity and is more than an order of magnitude shorter for the compact cavity ($r_i = 1$ mm).

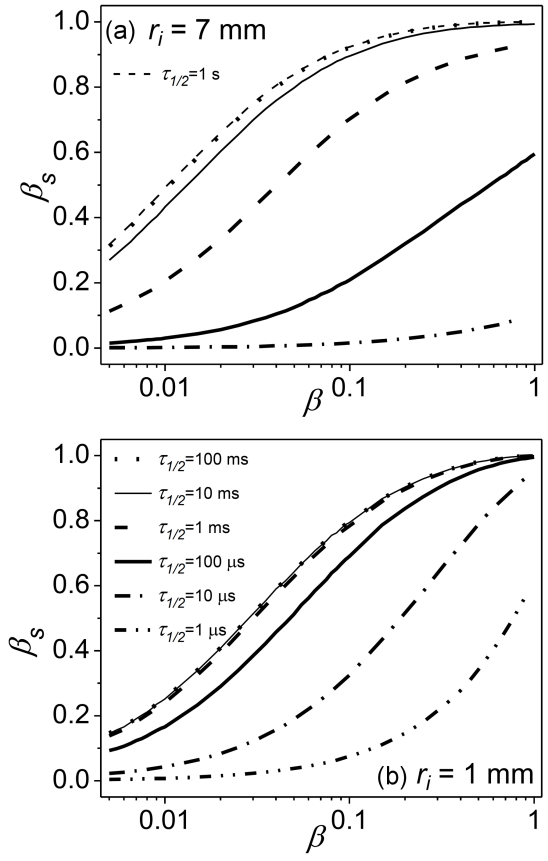

Fig. 2. Influence of nuclide half-life on the ion source ionization efficiency in the case of a flat disc cavity (a) and a compact cavity (b).

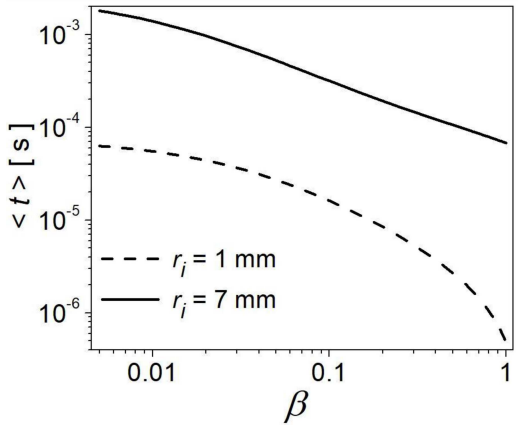

Fig. 3. Average flight times of particles inside both considered cavity configurations.

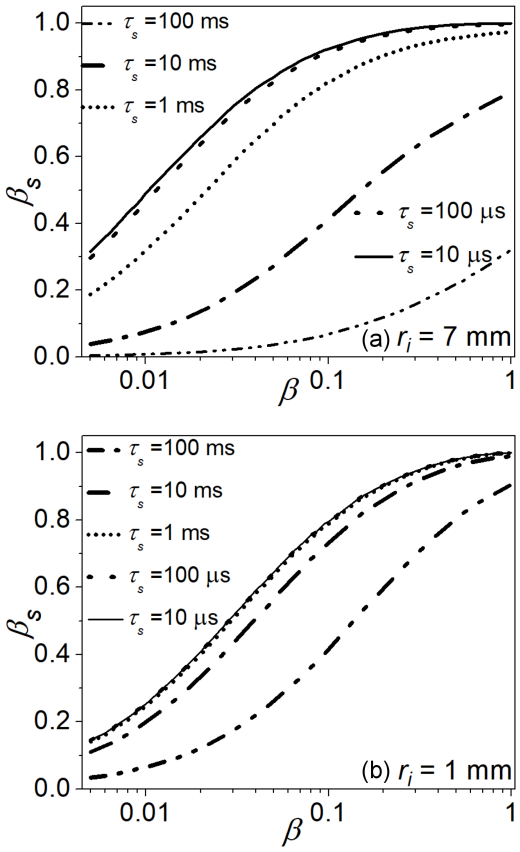

Fig. 4. Influence of the average particle–wall sticking time on the ion source ionization efficiency in the case of a flat disc cavity (a) and a compact cavity (b).

This is due to the fact that in the case of a compact cavity, the particle undergoes a smaller number of collisions with the ionizer walls than in the case of a thin and wide cavity. Moreover, one can see a rapid reduction of $\langle t \rangle$ — it reaches values near 5 μs for the latter case when β is close to 1 (easy-to-ionize substances).

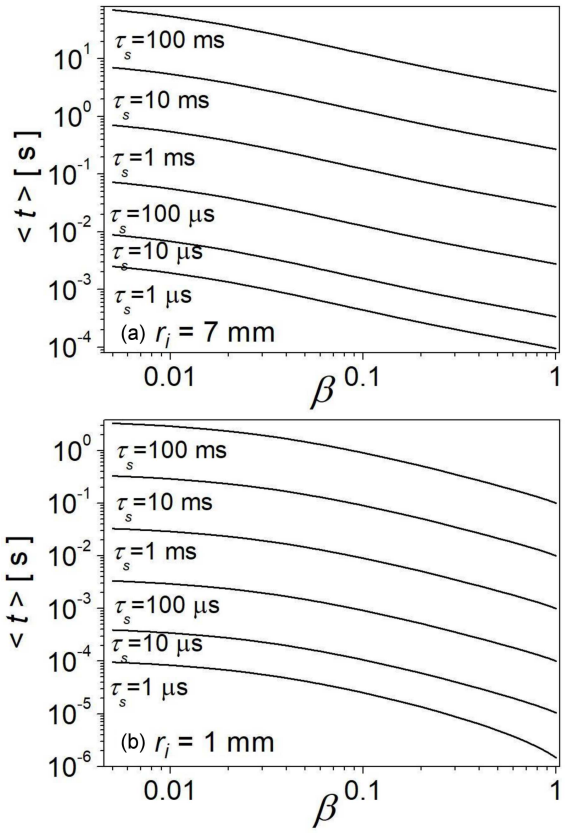

Fig. 5. Average time a particle stays inside the ionizer for the different sticking times τ_s.

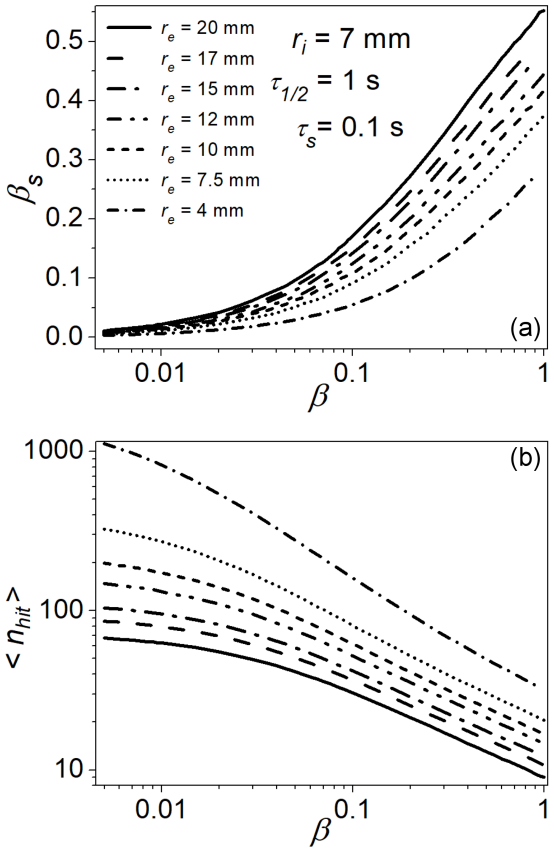

Fig. 6. The influence of the extraction opening radius on the ionization efficiency inside the flat disc cavity (a) and the average particle–wall collision numbers for the considered cases (b).

This difference has a great impact on the dependence of the $\beta_s(\beta)$ curves on the nuclide half-life. In the case of a flat disc cavity, one can see a deterioration of the efficiency for times $\tau_{1/2} = 1$ ms and shorter. On the other hand, most of the curves for longer half-lives behave similarly to the case of stable isotopes. A reduction of ionization efficiency by an order of magnitude can be observed for hard-to-ionize substances (small β) in the case of $\tau_{1/2} = 10$ μs. In turn, for β close to 1, this effect is rather small and becomes significant for extremely short-lived isotopes.

The difference between the two configuration mentioned above can be even better seen in the case of simulations results taking into account the delay due to particle sticking. Calculations were performed for $\tau_{1/2} = 1$ s, all other parameters were left unchanged. As one can see in Fig. 4, the influence of particle sticking delays is much stronger in the case of a flat disc cavity. Because particles undergo tens or even hundreds of collisions with hot walls, the total average time they spend in the cavity can reach even several tens of seconds (see $\langle t \rangle$ values presented in Fig. 5).

One should notice that in every case, $\langle t \rangle$ decreases with the ionization coefficient — the sooner the neutral atom is ionized, the sooner it will be extracted. As one can expect, the $\langle t \rangle$ values are by more than an order of magnitude shorter in the case of $r_i = 1$ mm. Even for a very long average sticking time ($\tau_s = 0.1$ s), the total time inside the cavity is of the same order as the nuclide half-life. This must lead to much better performance of the compact cavity in the case of short-lived nuclides, especially when their delays due to sticking are large. Figure 4a shows that a noticeable decrease of ionization efficiency is observed for τ_s of the order of 0.1 s. On the other hand, the performance of the flat disc cavity decreases rapidly for τ_s of the order of several milliseconds.

A good way to improve the ionization efficiency of the flat disc configuration in the case of short-lived substances is to increase the diameter of the extraction opening r_e. The results of calculations performed for r_e increasing from 4 up to 20 mm are shown in Fig. 6a. The timescales $\tau_{1/2}$ and τ_s were set as 1 s and 100 ms, respectively. One can see that increasing the size of the extraction opening in the above-mentioned range results in an improvement of the ionization efficiency more than twice. This is due to the fact that the wider extraction opening (i) makes the extraction of the produced ions much easier due to the better penetration of

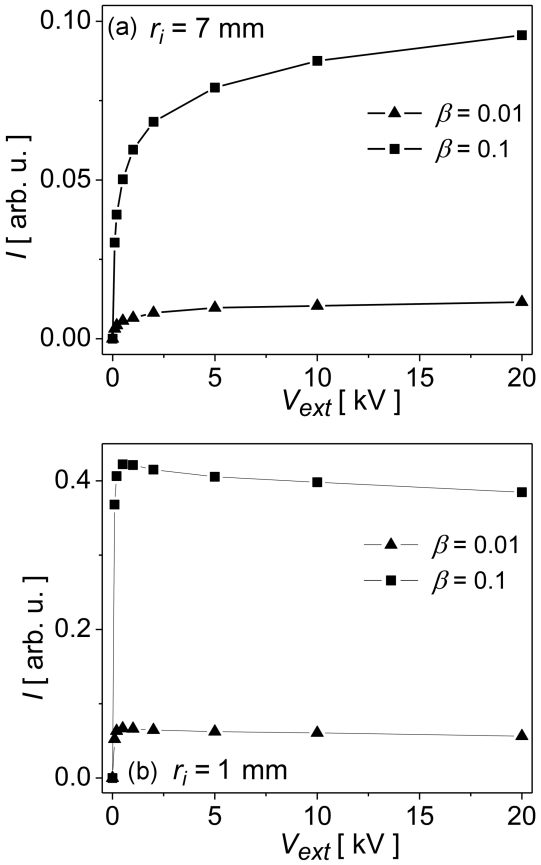

Fig. 7. Current–voltage curves calculated for a flat disc cavity (a) and compact cavity (b) of ionizer.

the electric field and, thus, (ii) reduces the possibility of ions neutralization during collisions and (iii) significantly decreases the time a particle stays inside the ionizer because the number of collisions is smaller and the average time inside the cavity is shorter, which consequently leads to the reduction of losses due to radioactive decay. Figure 6b shows that the average number of particle–wall collisions $\langle n_{hit} \rangle$ decreases by more than an order of magnitude when r_e increases from 4 up to 20 mm. However, one must keep in mind that the above-described mechanism works very well in the case of easy-to-ionize substances (characterized by large β). For hard-to-ionize substances, one deals with two concurrent tendencies. On the one hand, the ionization probability decreases for larger r_e as the number of collisions with a hot surface becomes smaller. On the other hand, losses due to decay become less important for a larger extraction opening. Hence, a trade-off between the two mentioned trends has to be found.

Figure 7 presents the current–voltage characteristics for the two considered cavity shapes. Simulations were performed for $\tau_{1/2} = 1$ s and $\tau_s = 100$ ms. The extraction voltage was increased up to 20 kV in both cases. Different shapes of the current–voltage curves can be observed. For a flat disc cavity, one can see a very rapid increase of the extracted current up to $V_{ext} = 2$ kV, while the increase of the yield above that value is rather slow. On the other hand, there is an even more rapid increase of the extracted current in the case of $r_i = 1$ mm, for V_{ext} up to 0.5 kV, followed by saturation and even a slight decrease of the current compared to the optimal value. The differences are due to the shape of the cavities. In the latter case, the extraction field penetrates a large part of the cavity even in the case of the moderate V_{ext} values, while for a very broad cavity, larger extraction potentials make the field reach deeper lying regions and capture more and more charged particles.

4. Conclusions

The numerical model of ionization in a disc-shaped cavity was presented in the paper. The model takes into account the nuclide losses due radioactive decay as well as delays related to the particle sticking to the hot ionizer walls. Two different shapes of the ionizer cavity were studied. A flat disc cavity with a large diameter seems much more suitable for stable but hard-to-ionize substances, as its shape makes the average number of collisions with the walls an order of magnitude higher than in the case of a compact cavity ($r_i = 1$ mm). On the other hand, a compact cavity is superior for short-lived isotopes, as the ions produced are extracted out of the cavity very fast. This is especially important for substances with a long average particle–wall sticking time. It was proved that the efficiency of the compact cavity is almost unaffected by sticking delays for τ_s up to 10 ms. The influence of the size of the extraction opening was also under investigation. It was found that enlarging the extraction channel diameter is a very simple way to increase the efficiency of the flat disc cavity for the short-lived nuclides, especially those with a small β coefficient. The current–voltage curves obtained for both configurations are characterized by different shapes. In the case of a compact cavity, one observes a fast increase followed by saturation, while in the case of a flat disc cavity, an increase of extraction voltage induces larger current though this effect is weaker for $V_{ext} > 2$ keV. The optimal value of the extraction voltage for a compact cavity is near 0.5 kV, while for a flat disc cavity, such value is much higher, approximately 2 kV.

References

[1] G.J. Beyer, E. Herrmann, A. Piotrowski, V.I. Raiko, H. Tyroff, *Nucl. Instrum. Methods* **96**, 437 (1971).

[2] P.G. Johnson, A. Bolson, C.M. Henderson, *Nucl. Instrum. Methods* **83**, 106 (1973).

[3] A. Latuszyński, K. Zuber, J. Zuber, A. Potempa, W. Żuk, *Nucl. Instrum. Methods* **120**, 321 (1974).

[4] D. Studer, L. Maske, P. Windpassinger, K. Wendt, *Phys. Rev. A* **98**, 042504 (2018).

[5] Y. Hirayama, Y.X. Watanabe, M. Mukai et al., *Nucl. Instrum. Methods Phys. Res. B* **463**, 425 (2020).

[6] Y. Duan, R.E. Danen, X. Yan, R. Steiner, J. Cuadrado, D. Wayne, V. Majidi, J.A. Olivares, *J. Am. Soc. Mass Spectrom.* **10**, 917 (1999).

[7] C. Maden, A. Trinquier, A.-L. Fauré, A. Hubert, F Pointurier, J. Rickli, B. Bourdon, *Int. J. Mass Spectrom.* **434**, 70 (2018).

[8] Y. Liu, C.U. Jost, A.J. Mendez II et al., *Nucl. Instrum. Methods Phys. Res. B* **298**, 5 (2013).

[9] N. Lecesne, *Rev. Sci. Instrum.* **83**, 02A916 (2012).

[10] J.L. Henares, N. Lecesne, L. Hijazi et al., *Nucl. Instrum. Methods Phys. Res. A* **830**, 520 (2016).

[11] R.Li J.Lassen, P. Kunz, M. Mostamand, B.B. Reich, A. Teigelhöfer, H. Yan, F. Ames, *Spectrochim. Acta Part B: At. Spectrosc.* **158**, 105633 (2019).

[12] K. Chrysalidis, J. Ballof, Ch.E. Düllmann et al., *Eur. Phys. J. A* **55**, 173 (2019).

[13] C. Babcock, T. Day Goodacre, A.Gottberg, *J. Phys. Conf. Series* **1067**, 052019 (2018).

[14] G.D. Alton, Y. Liu, D.W. Stracener, *Rev. Sci. Instrum.* **77**, 03A711 (2006).

[15] U. Köster, O. Arndt, E. Bouquerel et al., The TARGISOL Collaboration, *Nucl. Instrum. Methods Phys. Res. B* **266**, 4229 (2008).

[16] H.J. Woo, B.H. Kang, K. Tshoo, C.S. Seo, W. Hwang, Y.-H. Park, J.W. Yoon, S.H. Yoo, Y.K. Kim, D.Y. Jang, *J. Korean Phys. Soc.* **66**, 443 (2015).

[17] L. Popescu, EPFJ *Web of Conf.* **66**, 10011 (2014).

[18] V.G. Kalinnikov, K.Ya. Gromov, M. Janicki, Yu.V. Yushkevich, A.W. Potempa, V.G. Egorov, V.A. Bystrov, N.Yu. Kotovsky, S.V. Evtisov, *Nucl. Instrum. Methods Phys. Res. B* **70**, 62 (1992).

[19] L. Zhai, H. Deng, G. Wei, Z. Li, C. Wang, X. Li, G. Zhou, Y. Su, Z. Zhang, *Int. J. Mass Spectrom.* **305**, 45 (2011).

[20] G.D. Alton, Y. Zhang, *Nucl. Instrum. Methods Phys. Res. A* **539**, 540 (2005).

[21] G.D. Alton, Y. Liu, H. Zaim, S.N. Murray, *Nucl. Instrum. Methods Phys. Res. B* **211**, 425 (2003).

[22] P.A. Hausladen, D.C. Weisser, N.R. Lobanov, L.K. Fifield, H.J. Wallace, *Nucl. Instrum. Methods Phys. Res.* **190**, 402 (2002).

[23] A. Latuszyński, V.I. Raiko, *Nucl. Instrum. Methods* **125**, 61 (1975).

[24] M. Huyse, *Nucl. Instrum. Methods Phys. Res.* **215**, 1 (1983).

[25] R. Kirchner, *Nucl. Instrum. Methods Phys. Res. A* **292**, 203 (1990).

[26] A. Latuszyński, K. Pyszniak, A. Droździel, M. Turek, D. Mączka J. Meldizon, *Vacuum* **81**, 1150 (2007).

[27] M. Turek, K. Pyszniak, A. Drozdziel, J. Sielanko, *Vacuum* **82,** 1103 (2008).

[28] M. Turek, K. Pyszniak, A. Droździel, *Vacuum* **83**, S260 (2009).

[29] M. Turek, *Acta Phys. Pol. A* **123**, 847 (2013).

[30] M. Turek, A. Drozdziel, K. Pyszniak, D. Maczka, B. Slowinski, *Rev. Sci. Instrum.* **83**, 023303 (2012).

[31] M. Turek, *Acta Phys. Pol. A* **120**, 188 (2011).

[32] M. Turek, *Acta Phys. Pol. A* **128**, 935 (2015).

[33] M. Turek, *Acta Phys. Pol. A* **128**, 931 (2015).

[34] M. Turek, *Acta Phys. Pol. A* **132**, 259 (2017).

[35] M. Turek, *Przegląd Elektrotechniczny* **94**, 66 (2018).

[36] M. Turek, *Acta Phys. Pol. A* **136**, 329 (2019).

[37] M. Turek, *Vacuum* **104**, 1 (2014).

[38] M. Turek, *Devices Methods of Meas.* **11**, 132 (2020).

[39] M. Turek, J. Sielanko, P. Franzen, E. Speth, *AIP Conf. Proc.* **812**, 153 (2006).

[40] M. Turek, A. Drozdziel, K. Pyszniak, S. Prucnal, J.Żuk, *Przeglad Elektrotechniczny* **86** 193 (2010).

[41] A. Pyszniak, A. Droździel, M. Turek, A. Latuszyński, D. Maczka, J. Sielanko, Yu.A. Vaganov, Yu.V. Yushkevich, *Instrum. Exp. Techniq.* **50**, 552 (2007).

[42] M. Turek, J. Sielanko, *Vacuum* **83**, S256 (2009).

[43] B. Eichler, S. Htibener, H. Rossbach, *Zentralinstitut fur Kernforschung Rossendorf Report Reports* no. 560 and 561, 1985.